IEEE Access
Multidisciplinary | Rapid Review | Open Access Journal

Received May 29, 2019, accepted June 18, 2019, date of publication June 26, 2019, date of current version July 15, 2019.

Digital Object Identifier 10.1109/ACCESS.2019.2925136

Optimized Structure for a Moisture-Sensitive Colorimetric Sensor Utilizing Photonic Crystals Based on a Metal–Organic Framework

JUN YONG KIM, SUNG-HAK LEE, AND YUN SEON DO
School of Electronics Engineering, Kyungpook National University, Daegu 41566, South Korea
Corresponding author: Yun Seon Do (yuns.do@knu.ac.kr)

This work was supported by the Basic Science Research Programs through the National Research Foundation of Korea (NRF), Ministry of Education, under Grant NRF-2018R1D1A1B07045853, and 2009-0082580.

ABSTRACT We propose an optimized structure for a humidity-sensing colorimetric sensor that utilizes a metal-organic framework to form a one-dimensional photonic crystal. The structure changes spectral reflectivity by switching its photonic band gap (PBG). We found that, although photonic crystals on a highly reflective substrate increased the peak more than a transparent substrate, the resulting ripples in the wavelength band near the PBG destroy our ability to detect the color conversion. We also show that, despite the blue-shift of the peak PBG wavelength for higher angles of incidence, our sensor can still create significant color conversion at nonzero angles when the environmental humidity changes. Therefore, photonic crystals on a transparent substrate that utilize PBG-switching can operate as moisture-sensitive colorimetric sensors. Our study will help optimize sensors and industrial nano-structures.

INDEX TERMS Color, moisture, nanophotonics, optical sensors, photonic crystals.

I. INTRODUCTION

Photonic crystals (PhCs) exhibit a photonic band gap (PBG) due to periodic changes in their dielectric materials. The PhC structure reflects a specific wavelength band based on the PBG. Depending on the structure of the periodic array, PhCs are classified as one-dimensional (1D), two-dimensional (2D), or three-dimensional (3D) [1], [2]. By adjusting the optical properties of the PBG, sensors can be designed in two ways: by selecting materials with high refractive index sensitivity to environmental changes [3]–[5] or by changing the structure and size of the PhCs via external pressure [6]–[8]. By tailoring these optical properties, PhCs have been used in a variety of sensor applications, such as vapors [9]–[11], biological [13]–[15], solvent [5], [16], [17], ionic [18], [19], and temperature [20]–[22]. PhCs are particularly suited for colorimetric sensors, which measure visible color variations as the sensor environment changes since PhCs can create low-power, low-cost sensors [23].

Researchers have studied metal–organic frameworks (MOFs) as a way to enhance the performance of humidity sensors [24]–[26]. In this paper, we utilized a MOF as a moisture-sensitive material. A MOF is a porous polymer material composed of metal ions that are contained by an organic ligand. MOFs have larger pore volumes and higher surface areas than other nanoporous materials and can adsorb significant volumes of water. For example, the surface area of a MOF developed by the Hong Kong University of Science and Technology (HKUST-1) is 1502 (Brunauer-Emmett-Teller (BET)) and 2216 (Langmuir) m^2g^{-1} with a pore volume of 0.76 cm^3g^{-1}. In addition, this material can adsorb 40 wt% of water and its refractive index changes after exposure to a humid environment. Its excellent thermal stability allows reuse once the adsorbed water is removed at high temperatures [24], [27]–[30]. These properties led us to choose the HKUST-1 MOF material as an attractive candidate for a moisture sensor.

In this paper, we propose a humidity sensing colorimetric sensor that features a MOF material with a simple 1D photonic crystal structure. Existing research describes various sensors that utilize the spectral shifts of PBGs [9], [11], [12]. Here, we suggest a new method that focuses on switching the PBG instead of relying upon the PBG spectral shift. A previous study found that reflected light can be more

The associate editor coordinating the review of this manuscript and approving it for publication was Jiang Wu.

efficiently converted than transmitted light by environmental changes [31]. Based on this, we suggest an optimized structure for utilizing reflected light.

II. OPTIMIZED STRUCTURE FOR A MOISTURE-SENSITIVE COLORIMETRIC SENSOR

1D PhCs are optical materials consisting of periodic dielectrics or metal-dielectrics, in the form of Bragg stacks. The periodic change in the refractive indices of 1D PhCs creates a PBG, which affects propagation; the 1D PhC structure reflects the wavelengths of light that are blocked within the PBG [32]–[34]. The central wavelength of the PBG can be expressed by the interference of light occurring in the multilayer films, as defined by (1) [35].

$$d = \frac{\lambda}{4 \times n} \tag{1}$$

where d is the thickness of the material in the 1D PhC, λ is the central wavelength of the PBG, and n is the refractive index of each material in the 1D PhC. In (1), the central wavelength of the PBG depends on the thickness of the PhC materials and on changes in the refractive index. Therefore, we create a color representation of a 1D PhC structure with a PBG in the visible range by controlling the thicknesses and refractive indices of the PhC materials.

A previous study compared the color conversion of transmitted and reflected light by forming 1D PhCs on a glass substrate and found that the color conversion from reflected light was superior to the conversion from transmitted light [31]. We therefore chose to design a 1D PhC-based moisture-sensitive colorimetric sensor based on reflected light to derive the optimal structure.

We propose a design method to find the optimal reflected spectrum for the colorimetric sensor. Fig. 1 shows two concepts for a 1D PhC-based moisture-sensitive colorimetric sensor: a PhC structure formed on a transparent glass substrate (PCT) and a PhC structure formed on a highly- reflective substrate (PCR). We chose silver (Ag) as the highly reflective substrate. We expected that using a highly reflective substrate could affect the reflection spectrum of the structure, and could enhance the peak intensity of the PBG. In terms of its optical characteristics, Ag shows a relatively constant reflectivity in the visible light band and has less loss of reflected light than other reflective materials such as aluminum (Al) [36]. In this study, we designed the PCT and PCR structures and investigated how moisture affects the reflected light. The PCT structure is shown in Fig. 1(a) and the PCR structure is shown in Fig. 1(b).

After exposing the HKUST-1 powder to moisture, its crystal morphology and structure are observed by using a scanning electron microscope (SEM) and X-ray diffraction (XRD), there is no changed [37]. Since the thickness of the HKUST-1 film is not affected by moisture, we could focus on changes in its refractive index. The refractive indices according to the moisture content inside HKUST-1 were referred to the literature [38]. The refractive index of HKUST-1 increases

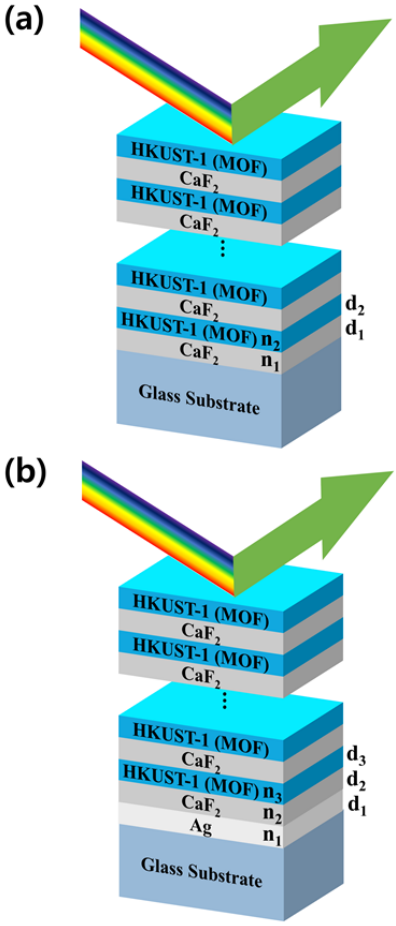

FIGURE 1. Two schematic designs for humidity-sensing colorimetric sensors based on a 1D PhC, formed on either (a) a transparent glass substrate or (b) a highly reflective substrate.

from about ∼1.44 to 1.55 at a wavelength of 450 nm when it is exposed to either ethanol (EtOH) or water. Also, the refractive index reduces with the drying condition of the HKUST-1 film. The higher drying temperature is the smaller value of the refractive index is shown, meaning the amount of adsorbed solvent is decreased. In this regard, the HKUST-1 film can be reusable and the amount of adsorbed solvent inside HKUST-1 film can be controlled by the drying temperature. The exact amount of adsorbed solvent inside HKUST-1 can be measured by the water-sorption kinetics [39]. When it is heated at a temperature of 200 °C for 18 hours, the refractive index returns to 1.44. Therefore, HKUST-1 and its applications can be reusable for water adsorbents. It can be expected from (1) that the central wavelength of the PBG changes when the refractive index of the material changes. In this way, a 1D PhC structure composed of HKUST-1 could result in the color conversion in visible light. Therefore, we chose HKUST-1 as the PhCs material with which to create a moisture-sensitive colorimetric sensor.

We compared the color transformations by using two optical methods. In the first, the PhC was combined of HKUST-1

and another material that has a different refractive index than bare HKUST-1 in the visible range. This method provides an opportunity to utilize the central wavelength shift of the PBG. To utilize the central wavelength shift of the PBG, we selected aluminum oxide (Al_2O_3).

The second method utilizes the PBG switch by using another material with the same refractive index as HKUST-1 in the visible range. The other material selected as calcium fluoride (CaF_2). In a dry environment, this combination does not create a PBG due to the small difference in the refractive indices of CaF_2 and HKUST-1. However, after being exposed to humidity, the material generates a PBG due to the relative increase in the difference between the refractive indices of CaF_2 and HKUST-1. All of the 1D PhCs were designed by constructing HKUST-1 and the other materials on either a glass or Ag substrate, as detailed above. On the substrate, the other optional material was deposited first, followed by HKUST-1; these were then stacked in turn.

The color system of the human eye can be expressed by the three primary colors of light [40]. To create a color conversion this is distinguishable by the naked eye, we aimed to represent the colors from the synthesis of the blue (400 nm), green (550 nm), and red (650 nm) wavelength bands. We designed devices for each wavelength band, defined as specific photonic bandgap-blue (SPB-B), green (SPB-G), and red (SPB-R). The thickness of the PhC materials (HKUST-1, CaF_2, and Al_2O_3) corresponding to SPB-B, SPB-G, and SPB-R, respectively, are shown in Table 1.

The HKUST-1 thin film can be grown using the liquid phase epitaxy (LPE) spray-coating method and the CaF_2 and Al_2O_3 thin films can be formed through atomic layer deposition (ALD) processes [38], [41], [42]. We calculated the required thickness of HKUST-1 using the refractive index when exposed to either EtOH or a humid environment. We fixed the thicknesses of each layer and changed only the refractive index of HKUST-1. We determined the thickness of the Ag layer that formed on the glass substrate to be 20 nm. At this thickness, Ag could be continuously deposited and could be grown as a perfect thin film [43].

We used the published experimental data for the refractive indices of the PhC materials and Ag [38], [44]–[46]. In equation (1), the central wavelength of a PBG depends on the refractive indices of PhC materials; these indices vary with wavelength. Considering this, we designed the optimized structures using the refractive index of each material at the central wavelength of the PBG. Table 2 summarizes the refractive indices of each material at the central wavelengths of SPB-B, SPB-G, and SPB-R.

A previous study compared color conversion by adjusting the number of 1D PhC layers formed on a glass substrate [31]. We found that ten pairs of 1D PhCs resulted in the best spectral change of SPB-G. We likewise formed ten pairs of 1D PhCs in the PCT and PCR structures for SPB-G, SPB-B, and SPB-R PhCs.

Using a 3D finite-difference time domain tool (FDTD Solutions by Lumerical Inc.), we measured the intensity of the reflected light in the z-axis direction of each of the structures shown in Fig. 1. To represent the infinite surface, we set boundary conditions that are anti-symmetric for the x-axis, symmetric for the y-axis, and perfectly matched layer (PML) for the z-axis. In addition, to observe the spectral changes as the incident light angle varies, we changed the boundary conditions of the x- and y-axes to Bloch. The light source incident on the 1D PhCs was a plane wave with wavelengths between 300 and 1000 nm. We placed a frequency-domain field monitor above the light source to measure the intensity of the reflected light.

TABLE 1. Calculated thicknesses of photonic crystal materials (in nm) for each wavelength.

Material	SPB-B (400 nm)	SPB-G (550 nm)	SPB-R (650 nm)
CaF_2	68	95	112
Al_2O_3	56	78	92
HKUST-1	64	90	108

TABLE 2. Defined refractive indices of photonic crystal materials for each wavelength.

λ (nm)	Ag	CaF_2	Al_2O_3	HKUST-1 (Dry)	HKUST-1 (Wet)
400	0.17 (Re) / 2.0 (Im)	1.44 (Re)	1.79 (Re)	1.47 (Re)	1.58 (Re)
550	0.13 (Re) / 3.3 (Im)	1.44 (Re)	1.77 (Re)	1.41 (Re)	1.53 (Re)
650	0.12 (Re) / 4.1 (Im)	1.43 (Re)	1.77 (Re)	1.40 (Re)	1.51 (Re)

III. RESULTS AND DISCUSSION

To verify the effects of the PBG changes, we first analyzed the spectrum changes. Fig. 2 shows the spectral changes according to each spectral shift and switch of PBG. The reflectance spectra of PhCs using the spectral shift and switch of PBG are shown in Figs. 2(a) and (b). Since the PhCs are not infinitely stacked, the main peak value of the PBG differ from each other. In addition, there are small ripples in the wavelength band, except for in the case of PBG. This phenomenon is caused by interference between multiple reflections at the finite boundary modes.

To take advantage of the shift in the PBG central wavelength, we selected HKUST-1 and Al_2O_3 as the PhCs materials in the PCT structure. The refractive index of Al_2O_3 differs from the refractive index of HKUST-1 both with and without moisture. The differences between the refractive indices of Al_2O_3 and HKUST-1 when dry were ∼0.32 (400 nm) and

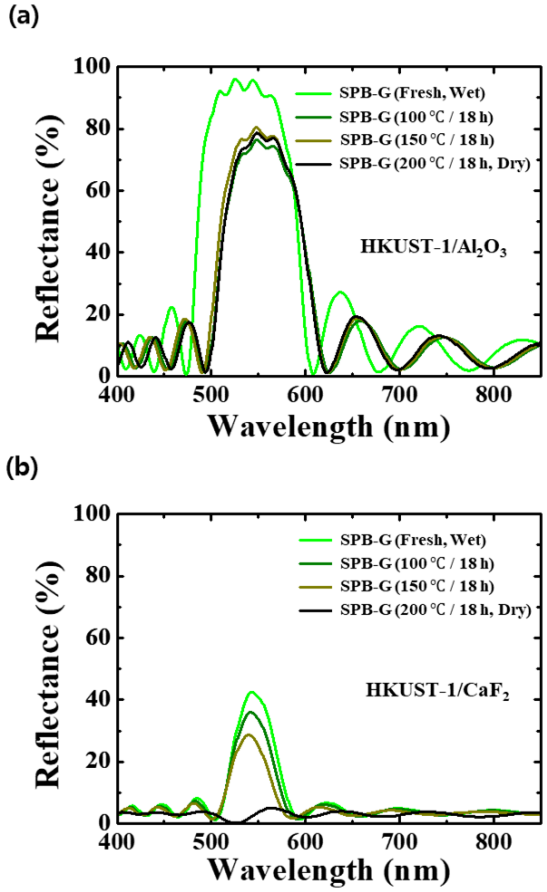

FIGURE 2. Spectral reflectivity of an HKUST-1 PCT structure with varying water content from (a) spectral shifts and (b) PBG switching.

∼0.37 (550 and 650 nm). For Al_2O_3 and HKUST-1 when freshly wet, the differences between these refractive indices were 0.21 (400 nm), 0.25 (550 nm), and 0.26 (650 nm). In both dry temperatures and wet conditions, the refractive index differences in these PhCs create a PBG. The shift in the PBG wavelength band is caused by the refractive index of HKUST-1 varying from wet to dry while the refractive index of Al_2O_3 remains constant. The wavelength band of PBG traveled ∼24 nm in the long wavelength band. The amount of spectral change according to the contents of adsorbed inside HKUST-1 was small. In addition, the spectrum's peak value decreased by ∼17%p because the difference in refractive indices decreased.

The spectral changes of PhCs in response to switching the PBG was distinct, however. In the dry environment, the reflected intensity of light in the overall spectral range was negligible. In addition, although a small peak was present in the PBG wavelength band, it was hardly distinguishable. Said a small peak is occurred due to the small difference between the refractive indices of CaF_2 and HKUST-1. In the wet environment, a PBG was present in the 550 nm wavelength band, because the difference in the refractive index between two materials increased. The average reflectance from 380 to 780 nm was calculated to be ∼3% in the dry environment, and the maximum peak value in the 500 to 600 nm wavelength band was as low as ∼5%. As the drying temperature increased in the wet condition, the maximum peak decreased sequentially to ∼43% (wet), 36% (100°C), 29% (150°C), and 5% (200°C, dry); the maximum peak in wet conditions is ∼8.5 times stronger than in dry conditions. Once we discovered that the spectral change created by switching the PBG was much stronger than by shifting the spectral peak, we selected a colorimetric sensor that utilized this PBG switching.

To enhance the main peak of the SPB-G while utilizing the PBG switch, we designed a PCR structure to compare with the PCT structure. Fig. 3 shows the spectral changes of PCT and PCR structures that both use PBG switching. We designed PCT and PCR structures for SPB-B, SPB-G, and SPB-R wavelengths and compared the spectral changes to understand their sensing performance.

Figs. 3(a), (b), and (c) show the reflectance spectra of SPB-B, SPB-G, and SPB-R that we designed with the PCT structure. The average reflectance between 380 and 780 nm in dry conditions was 3.6% (SPB-B), 3% (SPB-G), and 3.3% (SPB-R) and the maximum peak reflectance was ∼17% (380 nm), ∼5% (564 nm), and ∼6.4% (668 nm). In the humid environment, the peak reflected PCT intensities at the main central wavelength were ∼65% (396 nm), ∼43% (544 nm), and ∼36% (648 nm). Changing from dry to humid environments increased the maximum reflected light 3.9× (SPB-B), 8.5× (SPB-G), and 5.6× (SPB-R). Each of the dry environment samples had small peaks within the spectral range due to the small differences between the refractive indices of CaF_2 and HKUST-1; the refractive indices of HKUST-1 and CaF_2 in a dry environment are not perfectly identical between wavelengths of 380 to 780 nm. We observed refractive index differences of ∼0.03 (400, 550, and 650 nm) in each wavelength band.

We formed PhCs on PCR structures to enhance the maximum peak value of the central wavelength band and we compared these structures to the PhCs formed on PCT structures. Figs. 3(d), (e), and (f) show the spectral changes of the SPB-B, SPB-G, and SPB-R PhCs on PCR structures, respectively. In both dry and humid environments, the average reflected light intensities from the PCR structures were higher than the reflections from the PCT structures. In the SPB-B case, for example, the average reflectance increased from ∼3.6% to 55%. When the PCR structures were exposed to wet conditions, the maximum peak values in the central wavelength band only increased ∼1.3× (SPB-B), 2× (SPB-G), and 2.9× (SPB-R). Except for in the case of a PBG, however, severe ripples occurred in the wavelength band. When Ag, which has high reflectivity, was used as a substrate, most of the light was reflected, because the difference between the refractive indices of CaF_2 and Ag was large. Due to the difference in the refractive index between the PhCs and the air boundary, part of the light reflected from the Ag is reflected back into

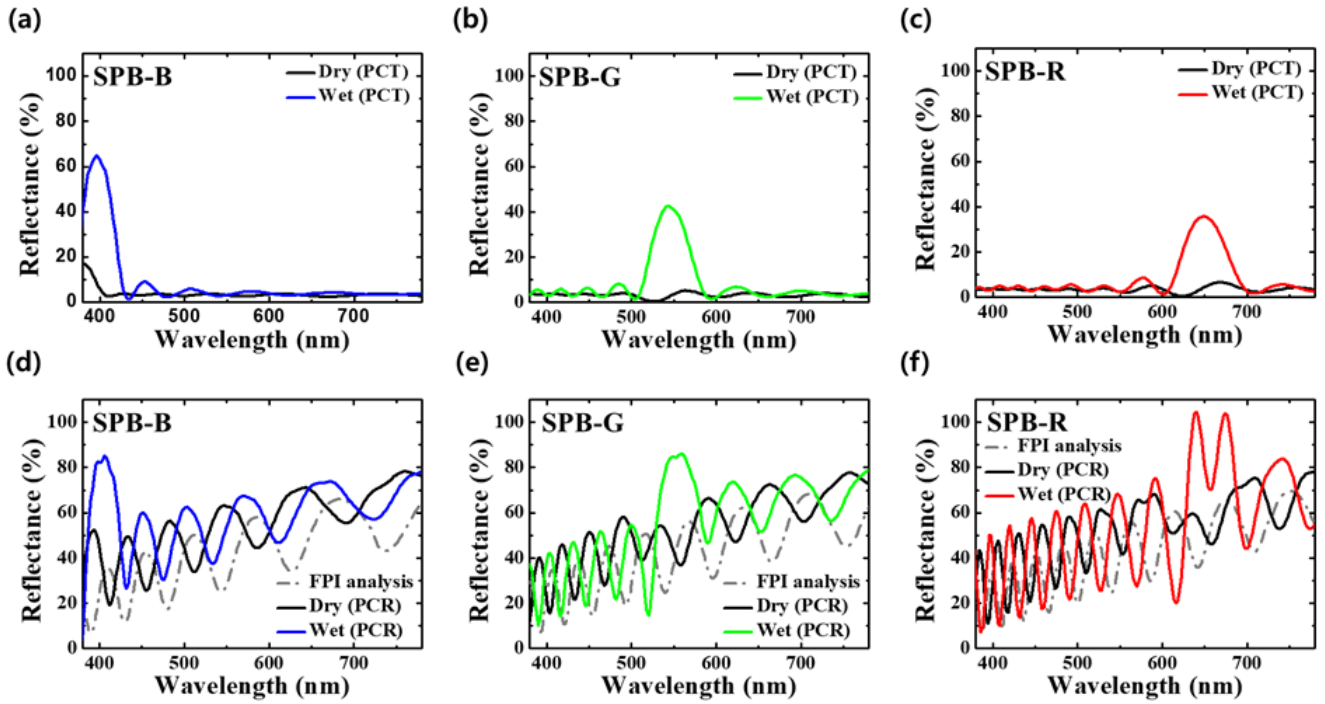

FIGURE 3. Spectral changes according to PCT and PCR structure of SPB-B, SPB-G, and SPB-R. (a), (b), and (c) show the PCT structures of SPB-B, SPB-G, and SPB-R, respectively, and (d), (e), and (f) show the PCR structures of each.

the PhCs. Repetition of this phenomenon means that the layers act as a Fabry-Perot interferometer (FPI), amplifying the effect of the PBG [47].

We analyzed the ripples in the PCR structures using the physical principles of an FPI. We constructed the FPI structures corresponding to SPB-B, SPB-G, and SPB-R by forming a material with a refractive index of 1.5 on a 20 nm Ag layer. For the refractive index of the material formed on the Ag layer, we used the average of HKUST-1 and CaF_2 refractive indices in the humid environment and we used thicknesses that correspond to the PhC thickness, which is 1320 nm for SPB-B, 1850 nm for SPB-G, and 2210 nm for SPB-R.

Figs. 3 (d), (e), and (f) show that the spectra of the FPI structures are similar to the spectra of the PCR structure in a wet environment: in a humid environment, SPB-B, SPB-G, and SPB-R see 5, 8, and 10 ripples, respectively, and the corresponding FPI structures see 5, 8, and 9 ripples. Since the peaks occur in similar wavelength regions, and the number of peaks is almost identical, we are confident that the ripples are generated by a Fabry-Perot effect in the PhCs between the Ag/PhC and PhC/air layers.

Furthermore, we can predict the wavelength between each the peaks by (2) using the physical principle of the free spectral range (FSR) [48], [49]:

$$\lambda_{FSR} = \frac{\lambda_0^2}{2nl} \tag{2}$$

where λ_0 is the central wavelength of peak and l and n are the thickness and average refractive index of the PhC, respectively. In (2), a thicker PhC will cause the FSR to decreases which implies a more severe ripple. Since SPB-R has the thickest stack of PhCs, it has the smallest FSR and the largest number of peaks in the visible spectrum. Likewise, the round trip through the PhCs increases the effective number of layers of 1D PhCs, which increases the central wavelength peak values of the PBG.

The difference in refractive indices between Ag and CaF_2 is ∼1.27, ∼1.31, and ∼1.31 in the 400, 550, and 650 nm wavelength bands, respectively. Since the refractive index differences in the 550 and 650 nm wavelength bands are larger than the difference in the 400 nm band, the intensity of the reflected light is more pronounced in the 550 and 650 nm wavelength bands.

Next, we compared the color conversion of the PCR and PCT structures using the International Commission on Illumination (CIE) 1976 $u'v'$ coordinate system. This system creates a uniform color space that reduces the non-uniformity between visual chrominance and color difference in the CIE 1931 xy coordinate system [50]. Figs. 4 (a), (b), and (c) show that the color coordinate shifts of the PCT and PCR structures of SPB-B, and SPB-G, and SPB-R shifted to blue, green, and red areas, respectively, when the environment was changed from the dry to the humid conditions. For the PCT structure, the color coordinates of each SPB-B, SPB-G, and SPB-R shifted from (0.21, 0.47), (0.23, 0.46), and (0.20, 0.47) to (0.21, 0.41), (0.14, 0.55), and (0.32, 0.49), respectively.

The PCR structure created much smaller moves: (0.22, 0.49), (0.23, 0.49), and (0.22, 0.50) to (0.22, 0.48), (0.22, 0.51), and (0.23, 0.49).

$$\Delta u'v' = \sqrt{(u'_1 - u'_2)^2 + (v'_1 - v'_2)^2}, Dry(u'_1, v'_1), Wet(u'_2, v'_2) \tag{3}$$

We also calculated the color coordinate shifts of the PCT and PCR structures quantitatively using (3). For the PCT structure, we calculated ∼0.06, ∼0.13, and ∼0.12 for $u'v'_{SPB-B}$, $u'v'_{SPB-G}$, and $u'v'_{SPB-R}$, respectively, whereas the PCR structure only changed by ∼0.01, ∼0.02 and ∼0.01. Since the PCT structure displayed much stronger color coordinate shifts than the PCR structure, we consider a PBG-switching PCT structure to be most suitable for a moisture-sensitive colorimetric sensor.

Fig. 5 shows the spectral and color coordinate changes of the optimized PCT structure for different incident angles. As the angle of incidence increases, the overall spectrum blue shifts in both dry and humid environments. Furthermore, when we increase the angle of incidence from 0° to 20°, the peak wavelength of the PBG decreases by ∼16 nm; the oblique incidence affects the reflected intensity and the transmission coefficients that occur at each PhC boundary. In addition, this phenomenon can be understood by the FPI physical principles: resonance occurs when the round trip phase difference of the wave vector (δ) is an integer multiple of 2π. In the case of oblique incidence, we can express the phase difference of the wave vector by (4) [51]:

$$\delta(\lambda, \theta) = 2kl\cos\theta = 2q\pi \tag{4}$$

where λ is the free-space wavelength, k is the wave number where $k = (2n\pi)/\lambda$, θ is the incident angle, q is an integer, and n and l are the refractive index and thickness of the material, respectively. In this equation, λ is affected by the angle of incidence.

When the central wavelength of the PBG shifts, the color coordinates shift as well. Fig. 5 (c) shows that, when the incident angle increases from 0° to 20° for the SPB-G PCT structure, the color coordinates shift from (0.23, 0.46) to (0.21, 0.46) in a dry environment and from (0.14, 0.55) to (0.10, 0.55) in a humid environment. This creates a $u'v'$ of ∼0.14 for an incident angle of 20° and the structure still creates color conversion when the environmental humidity changes.

Therefore, 1D PhCs formed in PCT structures and utilizing PBG switching are attractive as humidity colorimetric sensors. There are a variety of MOF materials that can adsorb large amounts of water as well as potentially evolving into water-absorbing agents through quantitative measurement of water content [39], [52]. We have selected an HKUST-1, which can be adsorbed enough water at relatively a lower pressure than other MOF materials [53]. Other highly adsorbent MOFs also can be used depending on the purpose. The maximum water content inside HKUST-1 can be adsorbed

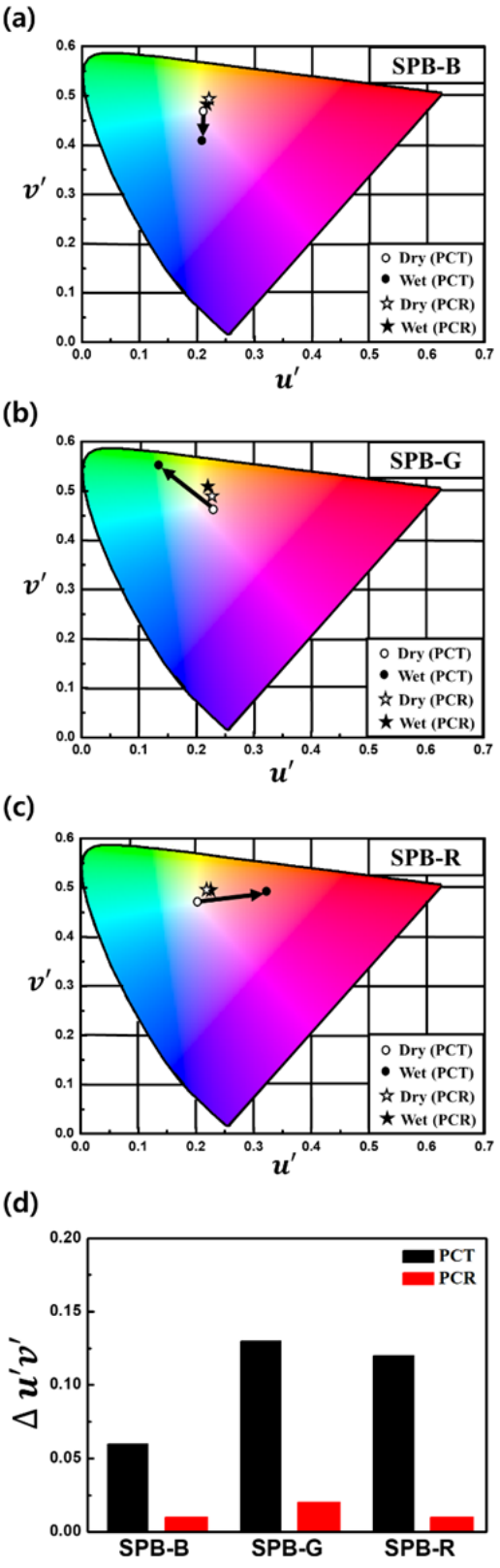

FIGURE 4. Color transformation between PCT and PCR structures in the CIE 1976 $u'v'$ coordinate system. (a), (b), and (c) show color conversion of the PCT and PCR structures of SPB-B, SPB-G, and SPB-R, respectively, and (d) shows the color shifts of each.

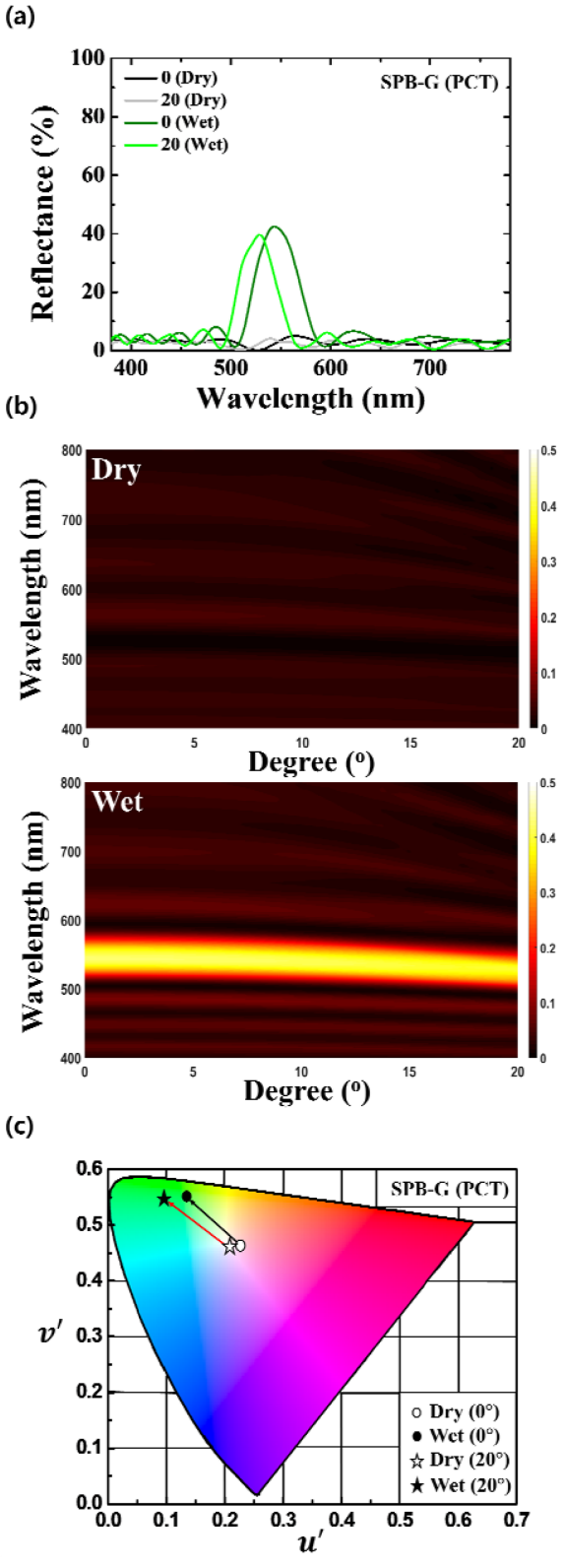

FIGURE 5. Spectral and color coordinate transformation vs. incident angle of the optimized PCT structure showing the (a) spectral response, (b) dispersion map of the reflection spectra, and (c) color shifts in the CIE 1976 $u'v'$ coordinate system.

from 43 to 65 wt%. Also, the EtOH can be adsorbed up to ∼45 wt% [54]. The water uptake of HKUST-1 saturates within 60 s at a vapor pressure of 5.9 mbar and a temperature of 36°C [55]. The colorimetric sensor that we d-esigned can be used as a sensor that directly creates a color change without a complicated or expensive detector.

IV. CONCLUSION

In this paper, we propose a moisture-sensitive colorimetric sensor that combines a simple 1D PhC on a PCT structure with a MOF that has good water adsorption. In the adsorption-desorption reaction of water or EtOH inside the HKUST-1 film, the spectral change of a switching PBG was clearer than the change from the spectral PBG shift. We also designed a PCR structure in an attempt to enhance the main peak of the PhCs in the PCT structure and, although the main peak value improved, the severe ripples in the wavelength bands near the PBG resulted in indistinguishable color conversion. We also determined that, while higher angles of incidence shift the peak PBG wavelength towards shorter wavelength, our structure still created color conversion when the environmental humidity increased. Therefore, we found the PCT structure, when utilizing a switching PBG, to be suitable as a moisture-sensitive colorimetric sensor. Our work will help optimize sensors and industrial nano-structures in the future.

ACKNOWLEDGMENTS

Authors would like to thank Professor J. H. Park for an in-depth discussion of materials research on MOFs.

REFERENCES

[1] K. Sakoda, *Optical Properties of Photonic Crystals*. Heidelberg, Germany: Springer, 2005, pp. 1–39.
[2] R. V. Nair and R. Vijaya, "Photonic crystal sensors: An overview," *Progr. Quantum Electron.*, vol. 34, no. 3, pp. 89–134, May 2010.
[3] Y. Zhao, Z. Xie, H. Gu, C. Zhu, and Z. Gu, "Bio-inspired variable structural color materials," *Chem. Soc. Rev.*, vol. 41, no. 8, pp. 3297–3317, Feb. 2012.
[4] I. Pavlichenko, A. T. Exner, M. Guehl, P. Lugli, G. Scarpa, and B. V. Lotsch, "Humidity-enhanced thermally tunable TiO_2/SiO_2 Bragg stacks," *J. Phys. Chem. C*, vol. 116, no. 1, pp. 298–305, Dec. 2012.
[5] S. Y. Choi, M. Mamak, G. Von Freymann, N. Chopra, and G. A. Ozin, "Mesoporous Bragg stack color tunable sensors," *Nano Lett.*, vol. 6, no. 11, pp. 2456–2461, Oct. 2006.
[6] B. Viel, T. Ruhl, and G. P. Hellmann, "Reversible deformation of opal elastomers," *Chem. Mater.*, vol. 19, no. 23, pp. 5673–5679, Oct. 2007.
[7] G. A. Ozin and A. C. Arsenault, "P-Ink and Elast-Ink from lab to market," *Mater. Today*, vol. 11, nos. 7–8, pp. 44–51, Jul./Aug. 2008.
[8] A. C. Arsenault, T. J. Clark, G. von Freymann, L. Cademartiri, R. Sapienza, J. Bertolotti, E. Vekris, S. Wong, V. Kitaev, I. Manners, R. Z. Wang, S. John, D. Wiersma, and G. A. Ozin, "From colour fingerprinting to the control of photoluminescence in elastic photonic crystals," *Nature Mater.*, vol. 5, no. 3, pp. 179–184, Mar. 2006.
[9] Z. Wang, J. Zhang, J. Xie, C. Li, Y. Li, S. Liang, Z. Tian, T. Wang, H. Zhang, H. Li, W. Xu, and B. Yang, "Bioinspired water-vapor-responsive organic/inorganic hybrid one-dimensional photonic crystals with tunable full-color stop band," *Adv. Funct. Mater.*, vol. 20, no. 21, pp. 3784–3790, Nov. 2010.
[10] Y. Kang, J. J. Walish, T. Gorishnyy, and E. L. Thomas, "Broad-wavelength-range chemically tunable block-copolymer photonic gels," *Nature Mater.*, vol. 6, no. 12, pp. 957–960, Dec. 2007.

[11] E. Tian, J. Wang, Y. Zheng, Y. Song, L. Jiang, and D. Zhu, "Colorful humidity sensitive photonic crystal hydrogel," *J. Mater. Chem.*, vol. 18, no. 10, pp. 1116–1122, Jan. 2008.
[12] S. Kim, A. N. Mitropoulos, J. D. Spitzberg, H. Tao, D. L. Kaplan, and F. G. Omenetto, "Silk inverse opals," *Nature Photon.*, vol. 6, no. 12, pp. 818–823, Dec. 2012.
[13] Y. Zhao, X. Zhao, and Z. Gu, "Photonic crystals in bioassays," *Adv. Funct. Mater.*, vol. 20, no. 18, pp. 2970–2988, Sep. 2010.
[14] Y.-J. Zhao, X.-W. Zhao, J. Hu, J. Li, W.-Y. Xu, and Z.-Z. Gu, "Multiplex label-free detection of biomolecules with an imprinted suspension array," *Angew. Chem. Int. Ed.*, vol. 48, no. 40, pp. 7350–7352, Sep. 2009.
[15] I. B. Burgess, L. Mishchenko, B. D. Hatton, M. Kolle, M. Lončar, and J. Aizenberg, "Encoding complex wettability patterns in chemically functionalized 3D photonic crystals," *J. Am. Chem. Soc.*, vol. 133, no. 2, p. 1374, Jan. 2012.
[16] W. Mönch, J. Dehnert, O. Prucker, J. Rühe, and H. Zappe, "Tunable Bragg filters based on polymer swelling," *Appl. Opt.*, vol. 45, no. 18, pp. 4284–4290, Jun. 2006.
[17] H. S. Lim, J.-H. Lee, J. J. Walish, and E. L. Thomas, "Dynamic swelling of tunable full-color block copolymer photonic gels via counterion exchange," *ACS Nano.*, vol. 6, no. 10, pp. 8933–8939, Sep. 2012.
[18] H. Saito, Y. Takeoka, and M. Watanabe, "Simple and precision design of porous gel as a visible indicator for ionic species and concentration," *Chem. Commun.*, vol. 3, no. 17, pp. 2126–2127, Jul. 2003.
[19] J. H. Holtz and S. A. Asher, "Polymerized colloidal crystal hydrogel films as intelligent chemical sensing materials," *Nature*, vol. 389, no. 6653, pp. 829–832, Oct. 1997.
[20] S. Kubo, Z.-Z. Gu, K. Takahashi, A. Fujishima, H. Segawa, and O. Sato, "Tunable photonic band gap crystals based on a liquid crystal-infiltrated inverse opal structure," *J. Am. Chem. Soc.*, vol. 126, no. 26, pp. 8314–8319, Jun. 2004.
[21] C. E. Reese, A. V. Mikhonin, M. Kamenjicki, A. Tikhonov, and S. A. Asher, "Nanogel nanosecond photonic crystal optical switching," *J. Am. Chem. Soc.*, vol. 126, no. 5, pp. 1493–1496, Jan. 2004.
[22] Y. Takeoka and M. Watanabe, "Template synthesis and optical properties of chameleonic poly(N-isopropylacrylamide) gels using closest-packed self-assembled colloidal silica crystals," *Adv. Mater.*, vol. 15, no. 3, pp. 199–201, Feb. 2003.
[23] M. M. Hawkeye and M. J. Brett, "Optimized colorimetric photonic-crystal humidity sensor fabricated using glancing angle deposition," *Adv. Funct. Mater.*, vol. 21, pp. 3652–3658, Oct. 2011.
[24] E. Biemmi, A. Darga, N. Stock, and T. Bein, "Direct growth of $Cu_3(BTC)_2(H_2O)_3$ ÂÛ xH_2O thin films on modified QCM-gold electrodes—Water sorption isotherms," *Microporous Mesoporous Mater.*, vol. 114, nos. 1–3, pp. 380–386, Sep. 2008.
[25] A. Douvali, A. C. Tsipis, S. V. Eliseeva, S. Petoud, G. S. Papaefstathiou, C. D. Malliakas, I. Papadas, G. S. Armatas, I. Margiolaki, M. G. Kanatzidis, T. Lazarides, and M. J. Manos, "Turn-on luminescence sensing and real-time detection of traces of water in organic solvents by a flexible metal–organic framework," *Angew. Chem.-Int. Ed.*, vol. 54, no. 5, pp. 1651–1656, Jan. 2015.
[26] Y. Yu, J.-P. Ma, and Y.-B. Dong, "Luminescent humidity sensors based on porous Ln^{3+}-MOFs," *CrystEngComm*, vol. 14, no. 21, pp. 7157–7160, Aug. 2012.
[27] Q. M. Wang, D. Shen, M. Bülow, M. L. Lau, S. Deng, F. R. Fitch, N. O. Lemcoff, and J. Semanscin, "Metallo-organic molecular sieve for gas separation and purification," *Microporous Mesoporous Mater.*, vol. 55, no. 2, pp. 217–230, Sep. 2002.
[28] I. Senkovska and S. Kaskel, "High pressure methane adsorption in the metal-organic frameworks $Cu_3(btc)_2$, $Zn_2(bdc)_2dabco$, and $Cr_3F(H_2O)_2O(bdc)_3$," *Microporous Mesoporous Mater.*, vol. 112, nos. 1–3, pp. 108–115, Jul. 2008.
[29] S. S. Y. Chui, S. M. Lo, J. P. Charmant, A. G. Orpen, and I. D. Williams, "A chemically functionalizable nanoporous material $[Cu_3(TMA)_2(H_2O)_3]n$," *Science*, vol. 283, no. 5405, pp. 1148–1150, Feb. 1999.
[30] M. D. Allendorf, R. J. T. Houk, L. Andruszkiewicz, A. A. Talin, J. Pikarsky, A. Choudhury, K. A. Gall, and P. J. Hesketh, "Stress-induced chemical detection using flexible metal-organic frameworks," *J. Am. Chem. Soc.*, vol. 130, no. 44, pp. 14404–14405, Oct. 2008.
[31] J. Y. Kim, S. H. Lee, and Y. S. Do, "Efficient humidity color sensor based on a photonic crystal with a metal-organic framework," *Korean J. Opt. Photon.*, vol. 29, no. 6, pp. 268–274, Dec. 2018.
[32] J. N. Winn, Y. Fink, S. Fan, and J. D. Joannopoulos, "Omnidirectional reflection from a one-dimensional photonic crystal," *Opt. Lett.*, vol. 23, pp. 1573–1575, Oct. 1998.
[33] J. D. Joannopoulos, P. R. Villeneuve, and S. Fan, "Photonic crystals," *Solid State Commun.*, vol. 102, nos. 2–3, pp. 165–173, Apr. 1997.
[34] Y.-K. Ha, Y.-C. Yang, J.-E. Kim, H. Y. Park, C.-S. Kee, and H. Lim, "Tunable omnidirectional reflection bands and defect modes of a one-dimensional photonic band gap structure with liquid crystals," *Appl. Phys. Lett.*, vol. 79, no. 15, Jun. 2001.
[35] J. M. Bendickson, J. P. Dowling, and M. Scalora, "Analytic expressions for the electromagnetic mode density in finite, one-dimensional, photonic band-gap structures," *Phys. Rev. E, Stat. Phys. Plasmas Fluids Relat. Interdiscip. Top.*, vol. 53, no. 4, p. 4107, Apr. 1996.
[36] M. N. Rashed, *Organic Pollutants-Monitoring, Risk and Treatment*. Rijeka, Croatia: InTech, 2013, ch. 2.
[37] B. H. Bowser, L. J. Brower, M. L. Ohnsorg, L. K. Gentry, C. K. Beaudoin, and M. E. Anderson, "Comparison of surface-bound and free-standing variations of HKUST-1 MOFs: Effect of activation and ammonia exposure on morphology, crystallinity, and composition," *Nanomaterials*, vol. 8, no. 9, p. 650, Aug. 2018.
[38] E. Redel, Z. Wang, S. Walheim, J. Liu, H. Gliemann, and C. Wöll, "On the dielectric and optical properties of surface-anchored metal-organic frameworks: A study on epitaxially grown thin films," *Appl. Phys. Lett.*, vol. 103, no. 9, Aug. 2013, Art. no. 091903.
[39] T.-Y. Tasi, P.-C. Wu, K.-T. Liao, H.-Y. Huang, C.-H. Lin, J.-S. Hsu, and W. Lee, "Purification of deteriorated liquid crystals by employing porous metal–organic-framework/polymer composites," *Opt. Mater. Express*, vol. 5, no. 3, pp. 639–647, Mar. 2015.
[40] G. Wyszecki and W. S. Stiles, *Color Science: Concepts and Methods, Quantitative Data and Formulae*, 2nd ed. New York, NY, USA: Wiley, 1982, ch. 2.
[41] T. Pilvi, K. Arstila, M. Ritala, and M. Leskelä, "Novel ALD process for depositing CaF_2 thin films," *Chem. Mater.*, vol. 19, no. 14, pp. 3387–3392, May 2007.
[42] M. D. Groner, J. W. Elam, F. H. Fabreguette, and S. M. George, "Electrical characterization of thin Al_2O_3 films grown by atomic layer deposition on silicon and various metal substrates," *Thin Solid Films*, vol. 413, nos. 1–2, pp. 186–197, Jun. 2002.
[43] K. H. Cho, S. I. Ahn, S. M. Lee, C. S. Choi, and K. C. Choi, "Surface plasmonic controllable enhanced emission from the intrachain and interchain excitons of a conjugated polymer," *Appl. Phys. Lett.*, vol. 97, no. 19, Nov. 2010, Art. no. 193306.
[44] S. Babar and J. H. Weaver, "Optical constants of Cu, Ag, and Au revisited," *Appl. Opt.*, vol. 54, no. 3, pp. 477–481, 2015.
[45] M. Daimon and A. Masumura, "High-accuracy measurements of the refractive index and its temperature coefficient of calcium fluoride in a wide wavelength range from 138 to 2326 nm," *Appl. Opt.*, vol. 41, no. 25, pp. 5275–5281, Sep. 2002.
[46] E. D. Palik, *Handbook of Optical Constants of Solids*, 1st ed. New York, NY, USA: Academic, 1998.
[47] N. Ismail, C. C. Kores, D. Geskus, and M. Pollnau, "Fabry-Pérot resonator: Spectral line shapes, generic and related Airy distributions, linewidths, finesses, and performance at low or frequency-dependent reflectivity," *Opt. Express*, vol. 24, no. 15, pp. 16366–16389, Jul. 2016.
[48] E. Hecht, *Optics*, 3rd ed. Reading, MA, USA: Addison-Wesley, 1998.
[49] D. G. Rabus, *Integrated Ring Resonators: The Compendium*. Berlin, Germany: Springer, 2007, ch. 2.
[50] G. Wyszecki and W. S. Stiles, *Color Science: Concepts and Methods, Quantitative Data and Formulae*. New York, NY, USA: Wiley, 1982, ch. 3.
[51] S. G. Lipson, H. Lipson, and A. Lipson, *Optical Physics*, 3rd ed. Cambridge, U.K.: Cambridge Univ. Press, 1995, ch. 9.
[52] C.-T. Huang, K.-T. Liao, C.-H. Lin, J.-S. Hsu, and W. Lee, "Improved electric properties of degraded liquid crystal using metal–organic frameworks," *Appl. Phys. Express*, vol. 6, no. 12, Nov. 2013, Art. no. 121701.
[53] M. J. Kalmutzki, C. S. Diercks, and O. M. Yaghi, "Metal–organic frameworks for water harvesting from air," *Adv. Mater.*, vol. 30, no. 37, Sep. 2018, Art. no. 1704304.

[54] J. R. Álvarez, E. Sánchez-González, E. Pérez, E. Schneider-Revueltas, A. Martínez, A. Tejeda-Cruz, A. Islas-Jácome, E. González-Zamora, and I. A. Ibarra, "Structure stability of HKUST-1 towards water and ethanol and their effect on its CO_2 capture properties," *Dalton Trans.*, vol. 46, no. 28, pp. 9192–9200, Jun. 2017.

[55] A. Rezk, R. Al-Dadah, S. Mahmoud, and A. Elsayed, "Experimental investigation of metal organic frameworks characteristics for water adsorption chillers," *Proc. Inst. Mech. Eng. C, J. Mech. Eng. Sci.*, vol. 227, no. 5, pp. 992–1005, May 2013.

JUN YONG KIM received the bachelor's degree from the Nano Photonics Applied Electronics Laboratory and the B.S. degree in electronics engineering from Kyungpook National University, Daegu, South Korea, in 2019, where he is currently pursuing the M.S. degree with the Nano Photonics Applied Electronics Laboratory, School of Electronics Engineering. From 2010 to 2012, he was with the Science Club, Danyang High School, where he performed science shows for children in kindergarten. He is currently studying nano-photonic structures for display devices and light emitting devices under the supervision of Prof. Y. S. Do. He published his first paper at the *Korean Journal of Optics and Photonics*, in 2018. He received an Award of Service in Seoul, in 2011.

SUNG-HAK LEE received the B.S., M.S., and Ph.D. degrees in electronics engineering from Kyungpook National University, in 1997, 1999, and 2008, respectively. He was with LG Electronics, from 1999 to 2004, as a Senior Research Engineer. He is currently an Assistant Professor with the School of Electronics Engineering, Kyungpook National University. His research interests include color management, color appearance model, HDR image processing, and display and image sensor applications for human visual systems.

YUN SEON DO was born in Daegu, South Korea, in 1983. She received the B.S. degree in electrical engineering from Kyungpook National University, Daegu, in 2005, and the M.S. and Ph.D. degrees in electrical engineering from KAIST, Daejeon, South Korea, in 2007 and 2013, respectively.

From 2007 to 2009, she was a Researcher with the Daegu Gyeongbook Institute of Science Technology (DGIST). She was also with Samsung Display, from 2013 to 2017, as a Senior Research Engineer with the Department of Frontier Technology. She is currently an Assistant Professor with the School of Electronics Engineering, Kyungpook National University. Her research interests include plasmonics, novel nanophotonic physics, active nanophotonic devices, and the electrical applications of such nanostructures for light emitting devices and solar energy devices, flexible and transparent displays, and light sensors (gas, bio, and robots).

Dr. Do was recipient of an Outstanding Poster Paper Award from the International Display Workshops, in 2006 and the Annual Honor Prize from the Department of Electrical Engineering, KAIST, in 2013. One of her research papers was selected as the Best of Advanced Optical Materials 2013.